PCCP

RSC Publishing

PAPER

Solution behaviors and microstructures of PNIPAm-P123-PNIPAm pentablock terpolymers in dilute and concentrated aqueous solutions†

Cite this: *Phys. Chem. Chem. Phys.*, 2013, **15**, 8276

Yanping Lu,[a] Tongquan Chen,[a] Aixiong Mei,[a] Tianyou Chen,[a] Yanwei Ding,[b] Xinghong Zhang,[a] Junting Xu,[a] Zhiqiang Fan[a] and Binyang Du*[a]

The solution behaviors and microstructures of poly(*N*-isopropylacrylamide)$_x$-poly(ethylene oxide)$_{20}$-poly(propylene oxide)$_{70}$-poly(ethylene oxide)$_{20}$-poly(*N*-isopropylacrylamide)$_x$ (PNIPAm$_x$-PEO$_{20}$-PPO$_{70}$-PEO$_{20}$-PNIPAm$_x$ or PNIPAm$_x$-P123-PNIPAm$_x$) pentablock terpolymers with various PNIPAm block lengths in dilute and concentrated aqueous solutions were investigated by micro-differential scanning calorimetry (micro-DSC), static and dynamic light scattering (SLS & DLS), and synchrotron small angle X-ray scattering (SAXS). Two lower critical solution temperatures (LCSTs) were observed for PNIPAm$_x$-P123-PNIPAm$_x$ pentablock terpolymers in dilute solutions, which corresponded to LCSTs of PPO and PNIPAm blocks, respectively. The LCST of PPO block shifted from 24.4 °C to 29 °C when the length *x* of PNIPAm block increased from 10 to 97. The LCST of PNIPAm is around 34.5 °C–35.3 °C and less dependent on the block length *x*. The PNIPAm$_x$-P123-PNIPAm$_x$ pentablock terpolymers formed ''associate'' structures and micelles with hydrophobic PNIPAm and PPO blocks as cores and soluble PEO blocks as coronas in dilute aqueous solutions at 20 °C and 40 °C, respectively, regardless of the relative lengths of PNIPAm, PPO and PEO blocks. The size of ''associate'' structures of PNIPAm$_x$-P123-PNIPAm$_x$ pentablock terpolymers at 20 °C increased with increasing the length of PNIPAm block. The microstructures of PNIPAm$_x$-P123-PNIPAm$_x$ hydrogels formed in concentrated aqueous solutions (40 wt%) were strongly dependent on the environmental temperatures and relative lengths of PNIPAm, PPO and PEO blocks as revealed by SAXS. Increasing the length of PNIPAm block weakened the order structures of PNIPAm$_x$-P123-PNIPAm$_x$ hydrogels. The microstructures of PNIPAm$_x$-P123-PNIPAm$_x$ hydrogels changed from mixed fcc and hex structures for PNIPAm$_{10}$-P123-PNIPAm$_{10}$ to isotropic structure for PNIPAm$_{97}$-P123-PNIPAm$_{97}$. Increasing temperature led to the transition from mixed hex and fcc structure to pure hex structure for PNIPAm$_{10}$-P123-PNIPAm$_{10}$ hydrogel at temperature above the LCSTs.

Received 26th January 2013,
Accepted 27th March 2013

DOI: 10.1039/c3cp50376c

www.rsc.org/pccp

Introduction

Multiblock copolymers with the number of blocks larger than three has attracted more and more research interest and attention in recent years, including synthesis methodologies, chain conformation, solution properties, adsorption behaviors of multiblock copolymers, and the like.[1–11] The structures of multiblock copolymers are thought to be close to those of biomacromolecules. The multiblock copolymers have multiple chain conformations. The studies of chain conformation and solution behavior of multiblock copolymers were thought to be helpful for understanding the solution properties of biomacromolecules. Furthermore, there are more control parameters, which could be used to tune the chain architectures of the multiblock copolymers. The different blocks could also have different functionalities. The structure–property relationship of multiblock copolymers might be then established *via* step-control of the chain architectures. Hence, the studies of synthesis, chain conformation, solution behavior, and related physical properties of multiblock copolymers are becoming an important research topic in the field of polymer science due to their scientific importance and potential applications.[1–11]

[a] *MOE Key Laboratory of Macromolecular Synthesis and Functionalization, Department of Polymer Science & Engineering, Zhejiang University, Hangzhou 310027, China. E-mail: duby@zju.edu.cn*

[b] *Hefei National Laboratory for Physical Sciences at Microscale, University of Science and Technology of China, Hefei, Anhui, China 230026*

† Electronic supplementary information (ESI) available: GPC traces of PNIPAm$_{10}$-P123-PNIPAm$_{10}$, PNIPAm$_{63}$-P123-PNIPAm$_{63}$, and PNIPAm$_{97}$-P123-PNIPAm$_{97}$ pentablock terpolymers, and representative ^{1}H-NMR spectrum of the PNIPAm$_{10}$-P123-PNIPAm$_{10}$ pentablock terpolymer. See DOI: 10.1039/c3cp50376c

The chain architecture and related physical properties of multiblock copolymers are much more complicated than those of diblock and triblock copolymers, which have been extensively studied from the aspects of fundamental research and technological applications.[12–17] The synthesis of multiblock copolymers with the block number >5 is still less controllable.[5,7,10] Therefore, pentablock copolymers with a block number of 5 were chosen as the simplest model systems for studying the structure and physical properties of multiblock copolymers because narrowly dispersed pentablock copolymers could be designed and synthesized by controlled radical polymerization techniques such as atomic transfer radical polymerization (ATRP), reversible addition–fragmentation transfer (RAFT) polymerization and the like.[2,18–27]

Mallapragada *et al.*[2,18,23] synthesized a series of pentablock terpolymers by ATRP with modified poly(ethylene oxide)$_{100}$-poly(propylene oxide)$_{65}$-poly(ethylene oxide)$_{100}$ (PEO_{100}-PPO_{65}-PEO_{100} or F127) macroinitiator and amine methacrylate as the monomer, including 2-(diethylamino)ethyl methacrylate (DEAEM), 2-(dimethylamino)ethyl methacrylate (DMAEM), 2-diisopropylaminoethyl methacrylate (DiPAEM), and (*tert*-butylamino)ethyl methacrylate (tBAEM). These authors found that such pentablock terpolymers formed thermo- and pH-responsive micelles in dilute aqueous solutions and pH-responsive, thermo-reversible hydrogels in concentrated aqueous solutions. Hadjiantoniou *et al.*[20] reported the formation of flower-like micelles for a pentablock copolymer of D_{20}-*b*-M_{10}-*b*-D_{20}-*b*-M_{10}-*b*-D_{20} in aqueous solution. Here, D and M were DEAEM and methyl methacrylate, respectively. Du *et al.*[22] showed that the pentablock terpolymer, $PNIPAm_{110}$-F127-$PNIPAm_{110}$, which was synthesized by ATRP with *N*-isopropylacrylamide (NIPAm) as the monomer and modified F127 as the macroinitiator, exhibited two lower critical solution temperatures (LCSTs) at 31 °C and 34 °C in the aqueous solution. The two LCSTs were attributed to the thermal phase transition of PPO block and PNIPAm block, respectively. Such pentablock terpolymer was thought to be meaningful for the construction of a thermo-responsive surface adsorption layer with a certain nanostructure on solid surface *via* varying the chain conformation in solution. Du *et al.*[9] further showed that the adsorption behaviors of $PNIPAm_{110}$-F127-$PNIPAm_{110}$ pentablock terpolymer on hydrophobic gold surfaces were indeed strongly dependent on the chain conformation in aqueous solution at different temperatures. Tsitsilianis *et al.*[26] synthesized poly(methyl methacrylate)–poly(acrylic acid)–poly(2-vinyl pyridine)–poly(acrylic acid)–poly(methyl methacrylate) (PMMA–PAA–P2VP–PAA–PMMA), ABCBA pentablock terpolymer by ''living'' anionic polymerization and found that such pentablock terpolymer exhibited rich association and gelation phenomena in aqueous solution with the presence of MeOH depending on the pH conditions of the aqueous solutions. The chain conformation, solution behavior and properties of the multiblock copolymers were also thought to be significantly affected by the relative lengths of blocks, numbers of blocks and chain architectures.[27] Lodge *et al.*[28] had showed that the critical gelation temperature (T_{gel}) for thermoreversible ion gels, which were prepared through the self-assembly of poly(*N*-isopropyl acrylamide-*b*-styrene-*b*-ethylene oxide-*b*-styrene-*b*-*N*-isopropyl acrylamide) (PNIPAm-PS-PEO-PS-PNIPAm) pentablock terpolymers in ionic liquid, could be adjusted over a significant range (17–48 °C) by varying the relative block lengths of PNIPAm and PS.

In order to understand the adsorption behavior on solid substrates and achieve the environmentally responsive surface layers with nanostructures, it is necessary and important to investigate the solution behavior of the environmental sensitive pentablock terpolymers not only in their dilute solutions but also in their concentrated solutions. In the present work, a series of thermally sensitive $PNIPAm_x$-PEO_{20}-PPO_{70}-PEO_{20}-$PNIPAm_x$ ($PNIPAm_x$-P123-$PNIPAm_x$) pentablock terpolymers with various length x of PNIPAm block were synthesized by the typical ATRP procedure with NIPAm as the monomer and modified P123 as the macroinitiator. The effects of relative block length and environmental temperatures on the solution behavior and microstructures of $PNIPAm_x$-P123-$PNIPAm_x$ pentablock terpolymers in dilute and concentrated aqueous solutions were investigated. The solution behaviors and chain conformation of $PNIPAm_x$-P123-$PNIPAm_x$ pentablock terpolymers in dilute aqueous solutions were first studied by using micro-differential scanning calorimetry (micro-DSC), static and dynamic light scattering (SLS & DLS). The information obtained from the dilute aqueous solutions was then correlated with the evolution of microstructures of the $PNIPAm_x$-P123-$PNIPAm_x$ hydrogel formed in concentrated aqueous solutions as a function of relative block length and environmental temperatures, which were investigated by using synchrotron small angle X-ray scattering (SAXS). The SAXS results showed that the incorporation of PNIPAm block strongly affected the microstructures of resultant $PNIPAm_x$-P123-$PNIPAm_x$ hydrogels, which were qualitatively discussed and explained in term of volume fraction, thermo-sensitive properties, Flory–Huggins interaction parameters and the interfacial curvatures of PPO, PEO and PNIPAm blocks in the hydrogels.

Experimental part

Chemical and materials

Pluronic P123 (PEO_{20}-PPO_{70}-PEO_{20}) with number averaged molecular weight M_n of 0.58×10^4 was a kind gift from BASF company. *N*-Isopropylacrylamide (NIPAm: 99%, ACROS ORGANICS) was recrystallized three times from toluene/hexane (1 : 1, v:v) prior to use. Three $PNIPAm_x$-P123-$PNIPAm_x$ pentablock terpolymers, namely $PNIPAm_{10}$-P123-$PNIPAm_{10}$, $PNIPAm_{63}$-P123-$PNIPAm_{63}$, and $PNIPAm_{97}$-P123-$PNIPAm_{97}$, were studied in the present work, which were synthesized by using a reported ATRP procedure with NIPAm as the monomer and modified P123 as the macroinitiator.[18,22] Note that x was the number of repeating unit of NIPAm and referred to the length of PNIPAm block. The chain structure, number average molecular weight M_n and molecular weight distribution M_w/M_n of the obtained pentablock terpolymers were characterized by ^{1}H-NMR and GPC, respectively, and are summarized in Table 1.

Table 1 Some physical parameters of $PNIPAm_x$-P123-$PNIPAm_x$ pentablock terpolymers

Pentablock terpolymers	M_n [a] ($\times 10^3$ g mol^{-1})	M_n [b] ($\times 10^3$ g mol^{-1})	M_w/M_n [b]	M_n [c] ($\times 10^3$ g mol^{-1})	M_w/M_n [c]
$PNIPAm_{10}$-P123-$PNIPAm_{10}$	8.3	8.9	1.25	11.4	1.34
$PNIPAm_{63}$-P123-$PNIPAm_{63}$	20.2	12.0	1.52	21.7	1.65
$PNIPAm_{97}$-P123-$PNIPAm_{97}$	28.0	16.5	1.44	29.3	1.69

[a] Determined from ^{1}H-NMR. [b] Determined from GPC with THF as eluent and monodisperse polystyrene as the calibration standard. [c] Determined from GPC with DMF and 0.05 M LiBr as eluent and monodisperse poly(methyl methacrylate) as the calibration standard.

Preparation of dilute and concentrated aqueous solution of pentablock terpolymers

Each pentablock terpolymer was dissolved in de-ionized water to give dilute aqueous solutions with concentrations of 5 mg mL^{-1} and 0.5 mg mL^{-1}, respectively. Concentrated aqueous solutions of P123 and $PNIPAm_x$-P123-$PNIPAm_x$ pentablock terpolymers, *i.e.* hydrogels, were prepared by dissolving the given polymers into de-ionized water until the polymer content reached 40 wt%. After complete dissolution of the given polymers, clear aqueous gels (40 wt%) of P123 and $PNIPAm_x$-P123-$PNIPAm_x$ pentablock terpolymers were obtained.

Instrumentation and characterization

Molecular weights and molecular weight distributions of $PNIPAm_x$-P123-$PNIPAm_x$ pentablock terpolymers were determined by using a gel permeation chromatograph (GPC, PL-GPC 220, Polymer Laboratories Ltd.) with tetrahydrofuran as the eluent and monodisperse polystyrene (PS) as the calibration standard. The molecular weight and molecular weight distribution of the pentablock terpolymer were also determined by using a Waters 1515 GPC (Waters Corporation) with DMF/0.05 M LiBr as eluent and monodisperse poly(methyl methacrylate) (PMMA) as the calibration standard. The number average molecular weights, M_n, was also determined from ^{1}H-NMR spectra of the pentablock terpolymers, which were obtained by using a 300 MHz Varian Mercury Plus NMR instrument with $CDCl_3$ as solvent and tetramethylsilane (TMS) as the internal standard. The GPC traces and representative ^{1}H-NMR spectrum of the pentablock terpolymers were shown in the ESI.† Note, from the data shown in Table 1, one can see that the M_n obtained by GPC with DMF/0.05 M LiBr as eluent and monodisperse PMMA as the calibration standard was closer to that determined by ^{1}H-NMR, whereas the M_n obtained by GPC with THF as eluent and monodisperse PS as the calibration standard was strongly deviated from that determined by ^{1}H-NMR especially for long PNIPAm block. The possible explanation might be the following: PNIPAm is a polar polymer, which can be dissolved well in the polar solvent of DMF. The PNIPAm chain will behavior more like a random coil in DMF. The polarity of THF is less than that of DMF so the PNIPAm chain will take a more compact chain conformation. Furthermore, PMMA is a polar polymer and better as the calibration standard for the polar polymers. As a result, the PNIPAm-P123-PNIPAm will exhibit a small molecular weight and narrow polydispersity in THF as shown in Table 1. Nevertheless, the GPC results showed that the obtained PNIPAm-P123-PNIPAm pentablock terpolymers exhibited relative narrow polydispersities.

Micro-differential scanning calorimetry (micro-DSC) measurements were carried out by using a VP DSC (MicroCal) in Hefei National Laboratory for Physical Sciences at Microscale, University of Science and Technology of China. Each pentablock terpolymer was dissolved in de-ionized water to give an aqueous solution with concentration of 5 mg mL^{-1}. The heating rate was 1.0 °C min^{-1}.

The static and dynamic light scattering (SLS and DLS) of the dilute aqueous solutions of the pentablock terpolymers (with concentration of 0.5 mg mL^{-1}) were carried out by using a Brookhaven Instrument BI-200SM with a laser wavelength of 636 nm and a temperature control unit. The temperature was precisely regulated *via* an external thermostat. Dust was removed from the solutions by filtering them through PES membrane filters of 0.22 μm pore size prior to measurements. Measurements were carried out at each temperature after the samples reached equilibrium. The DLS data were then analyzed by using free software AfterALV with the CONTIN routines to give the apparent hydrodynamic radius $\langle R_h \rangle$ and the distribution of $\langle R_h \rangle$.

The microstructures of aqueous gels of pentablock terpolymers (40 wt%) were investigated by using small angle X-ray scattering (SAXS) measurements, which were performed at BL16B1 of Shanghai Synchrotron Radiation Facility (SSRF). The X-ray wavelength was 0.124 nm, and a Mar165 CCD detector was employed to collect time-resolved two-dimensional (2D) SAXS patterns. The hydrogel samples were sandwiched with Kapton films for the SAXS measurements. The temperatures of the samples were controlled by a Linkam heating-cooling stage. The sample-to-detector distance was 2 m. The q scale was calibrated with collagen (beef tendon). Fit2D software from European Synchrotron Radiation Facility was used to analyze SAXS patterns and calculate the one-dimensional intensity profiles.

Results and discussion

Thermo-sensitive solution behaviors of pentablock terpolymers in dilute aqueous solutions

Fig. 1 shows the micro-DSC data curves of three $PNIPAm_x$-P123-$PNIPAm_x$ pentablock terpolymers in dilute aqueous solutions with the concentration of 5 mg mL^{-1} during the heating process. All of the three $PNIPAm_x$-P123-$PNIPAm_x$ pentablock terpolymers clearly exhibited two thermal transitions. $PNIPAm_{10}$-P123-$PNIPAm_{10}$ showed a bimodal transition with a strong endothermic peak centered at 24.4 °C and a small endothermic peak centered at 34.5 °C. With increasing the length of PNIPAm block from 10 to 63, *i.e.* $PNIPAm_{63}$-P123-$PNIPAm_{63}$, two endothermic peaks with comparable magnitudes were observed, which were centered at 26.5 °C and 35.3 °C. For the $PNIPAm_{97}$-P123-$PNIPAm_{97}$ with longest PNIPAm block length (x = 97), the micro-DSC data curve showed a bimodal transition with a

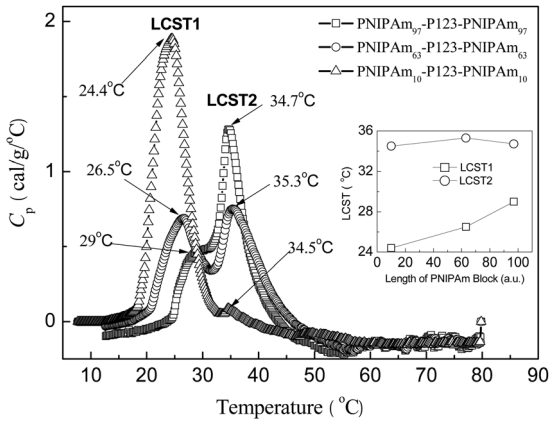

Fig. 1 Temperature dependence of the specific heat capacity (C_p) for the PNIPAm$_x$-P123-PNIPAm$_x$ pentablock terpolymers in aqueous solutions with concentration of 5 mg mL^{-1}. The inset shows the change of the two LCSTs as a function of length of PNIPAm block.

shoulder endothermic peak centered at 29 °C and a strong endothermic peak centered at 34.7 °C. Alexandridis *et al.* reported that P123 exhibited a LCST at 16 °C for 1 wt% aqueous solution, which was attributed to the PPO block.[29] For PNIPAm homopolymer, its LCST is around 32–34 °C in aqueous solution.[30–32] Therefore, the first and second endothermic peaks could be attributed to the LCSTs of PPO block and PNIPAm block, respectively, for PNIPAm$_x$-P123-PNIPAm$_x$ pentablock terpolymers. A similar phenomenon was previously observed for PNIPAm$_{110}$-F127-PNIPAm$_{110}$ pentablock terpolymer in dilute aqueous solution.[22] In our previous studies on PNIPAm$_{110}$-PEO$_{100}$-PPO$_{65}$-PEO$_{100}$-PNIPAm$_{110}$ (PNIPAm$_{110}$-F127-PNIPAm$_{110}$) pentablock terpolymer, a bimodal transition with a shoulder endothermic peak centered at 31 °C and a strong endothermic peak centered at 34 °C were observed, which had been attributed to the LCSTs of the PPO block and PNIPAm block, respectively.[22] Furthermore, Fig. 1 also shows that the magnitude of the first endothermic peak decreased with increasing the relative length of PNIPAm block, whereas the magnitude of the second endothermic peak increased with increasing the relative length of PNIPAm block. The inset of Fig. 1 shows the evolution of the endothermic peaks as the function of the PNIPAm block length. It can be seen that the first endothermic peak, *i.e.* corresponding to the LCST of PPO block, shifted to higher temperature with increasing the length of PNIPAm block. It meant that the LCST of PPO block of PNIPAm$_x$-P123-PNIPAm$_x$ was strongly dependent on the length of PNIPAm block. It was reasonable because the PNIPAm chain is hydrophilic at the temperature <34 °C, leading to the increase of LCST of PPO block. Note that the PEO block of P123 was only 20. The longer hydrophilic PNIPAm block was enchained, the higher LCST of PPO block was for PNIPAm$_x$-P123-PNIPAm$_x$. The second endothermic peak, *i.e.* corresponding to the LCST of PNIPAm, was less affected by the length of PNIPAm block. It was also understandable because the PEO and PPO blocks of P123 were the same for the three PNIPAm$_x$-P123-PNIPAm$_x$ pentablock terpolymers. For the PNIPAm$_{110}$-F127-PNIPAm$_{110}$ pentablock terpolymer, the LCST of PNIPAm block was 34 °C and similar to those observed here for PNIPAm$_x$-P123-PNIPAm$_x$ pentablock terpolymers.[22] Recently, Feng *et al.* reported the synthesis and aggregation behavior of similar thermo-responsive pentablock terpolymers PNIPAm-PEO-PPO-PEO-PNIPAm with various block lengths.[33] The authors synthesized a series of PNIPAm-PEO-PPO-PEO-PNIPAm pentablock terpolymers by RAFT polymerization with NIPAm as comonomer and Pluronic as macro-RAFT agents. The Pluronic macro-RAFT agents were synthesized by using *S*-1-dodecyl-*S*′-(α′,α′-dimethyl-α″-aceticacid)trithiocarbonate (DDAT) as chain transfer agent (CTA). They studied the effects of NIPAm and PPO block lengths on the LCSTs of the pentablock terpolymers, which were determined by UV-Vis spectrophotoscopy. They observed a single LCST for the PNIPAm-PEO-PPO-PEO-PNIPAm pentablock terpolymers studied and found that the LCST value decreased with increasing the hydrophobic NIPAm and PPO block lengths, which could be ascribed to the increase of attractive hydrophobic interactions of the pentablock terpolymers.[33] The micro-DSC results obtained here also indicated that the thermo-sensitive behaviors of the PNIPAm$_x$-P123-PNIPAm$_x$ pentablock terpolymers in the aqueous solutions were strongly dependent on the relative lengths of PNIPAm and PPO blocks.

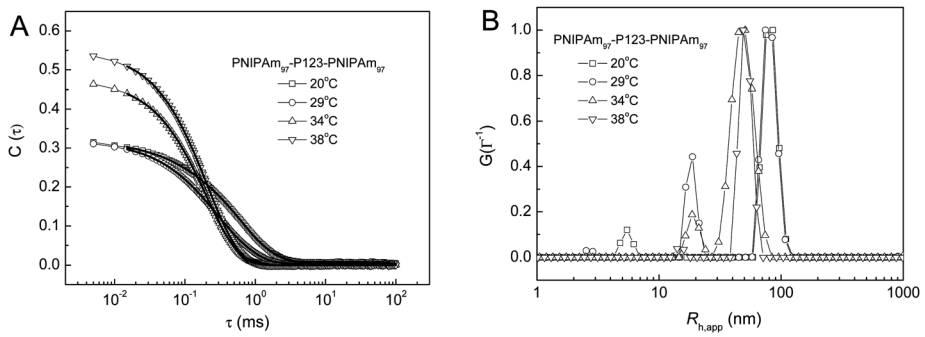

Fig. 2 (A) The autocorrelation function $C(\tau)$ measured by DLS for PNIPAm$_{97}$-P123-PNIPAm$_{97}$ aqueous solution with the concentration of 0.5 mg mL^{-1} at different temperatures, *i.e.* 20 °C, 29 °C, 34 °C and 38 °C. The solid lines are CONTIN fits. (B) The corresponding distribution of hydrodynamic radius $\langle R_h \rangle$ calculated by using CONTIN routine.

The chain conformation of PNIPAm$_x$-P123-PNIPAm$_x$ pentablock terpolymers in dilute aqueous solutions was further studied by dynamic light scattering (DLS). Fig. 2 shows the representative DLS autocorrelation functions $C(\tau)$s for PNIPAm$_{97}$-P123-PNIPAm$_{97}$ aqueous solution with the concentration of 0.5 mg mL^{-1} at different temperatures, *i.e.* 20 °C, 29 °C, 34 °C and 38 °C, and the corresponding distribution of hydrodynamic radius $\langle R_h \rangle$. At low temperature (*i.e.* 20 °C) where PNIPAm, PEO and PPO were well dissolved in aqueous solution, the bimodal distribution was observed with a larger $\langle R_h \rangle$ at *ca.* 83 nm and a smaller $\langle R_h \rangle$ at *ca.* 5.5 nm, indicating the existence of large "associate" structures for PNIPAm$_{97}$-P123-PNIPAm$_{97}$ molecular chains in the dilute aqueous solutions at 20 °C, which was similar to the previous report.[22] The smaller $\langle R_h \rangle$ could be assigned the single chain conformation of PNIPAm$_{97}$-P123-PNIPAm$_{97}$. Such "associate" structures have been observed for many PEO-containing block copolymers such PEO-*b*-PNIPAm and PEO-*b*-poly(*N*,*N*-dimethylacrylamide) (PEO-*b*-PDMA) in their dilute aqueous solutions at low temperature, at which the other block was soluble in water.[7,8,34,35] Liang *et al.*[34,35] supposed that the "associate" structures containing PEO-rich and PNIPAm-rich domains will be formed by the association of some PEO-*b*-PNIPAm chains at temperatures well below the LCST of PNIPAm due to the incompatibility between PNIPAm and PEO. Feng *et al.*[33] also observed the associated spherical-like particle structures formed by the similar PNIPAm-PEO-PPO-PEO-PNIPAm terpolymers in aqueous solution at temperature lower than the LCSTs of terpolymers, *i.e.* 25 °C. Since these PNIPAm-PEO-PPO-PEO-PNIPAm pentablock terpolymers were synthesized *via* RAFT polymerization using DDAT as chain transfer agent (CTA), they supposed that the formation of such "associate" structures were due to the association of the hydrophobic C_{12} chain at the end of the pentablock terpolymer, which was incompatible with PEO, PPO and PNIPAm blocks. When the temperature was increased to the first LCST of PNIPAm$_{97}$-P123-PNIPAm$_{97}$ at 29 °C, the single chain conformation disappeared and another peak centered at *ca.* 18 nm appeared (Fig. 2B). At 29 °C, the PPO block started to collapse, forming the micelles with PPO block as the cores and PNIPAM, PEO blocks as the coronas. With further increasing the temperature to the second LCST at 34 °C, the distribution peak centered at *ca.* 18 nm remained but with lower magnitude and the distribution peak of "associate" structures disappeared. Instead, another peak centered at *ca.* 47 nm appeared. Note that 34 °C was corresponding to the LCST of PNIPAm block. The PNIPAm blocks became hydrophobic and insoluble in water. The peak at 47 nm indicated the formation of micelles with PPO and PNIPAm blocks as the cores and PEO block as the coronas. These two peaks might suggest that the two types of micelles coexisted in the aqueous solution at 34 °C. At a temperature of 38 °C, well above the LCST of PNIPAm block, the first peak at *ca.* 18 nm disappeared and the peak at *ca.* 47 nm became narrow, indicating that all of the PNIPAm$_{97}$-P123-PNIPAm$_{97}$ molecular chains formed the micelles with PPO and PNIPAm blocks as the cores and PEO block as the coronas. Again, Feng *et al.*[33] also found that the similar PNIPAm-PEO-PPO-PEO-PNIPAm pentablock terpolymers formed the spherical micelles with PPO and PNIPAm as the cores and PEO as the shells at temperatures above their LCSTs. The evolution of distribution of hydrodynamic radius $\langle R_h \rangle$ as a function of temperature further supported the formation of large "associate" structures for PNIPAm$_{97}$-P123-PNIPAm$_{97}$ molecular chains in the dilute aqueous solutions at low temperature (20 °C).

Fig. 3 shows the distribution of hydrodynamic radius $\langle R_h \rangle$ of PNIPAm$_x$-P123-PNIPAm$_x$ pentablock terpolymers in dilute aqueous solutions with concentration of 0.5 mg mL^{-1} at 20 °C and 45 °C obtained by DLS at scattering angle of 90°. Clearly, the bimodal (or multimodal) distribution was observed at the temperature (20 °C) well below the LCSTs of the PPO and PNIPAm blocks for the three pentablock terpolymers (Fig. 3A), indicating the formation of "associate" structures" for the three PNIPAm$_x$-P123-PNIPAm$_x$ pentablock terpolymers regardless of the relative lengths of PNIPAm, PPO and PEO blocks. At temperature (45 °C) well above the LCSTs of the PPO and PNIPAm blocks, the PNIPAm$_x$-P123-PNIPAm$_x$ pentablock terpolymers formed micelles with uniform distribution regardless of the relative lengths of PNIPAm, PPO, and PEO blocks (Fig. 3B).

Fig. 4 shows the evolution of scattering intensity obtained by DLS at scattering angle of 90° for PNIPAm$_x$-P123-PNIPAm$_x$ pentablock terpolymers in dilute aqueous solutions with the concentration of 0.5 mg mL^{-1} as a function of temperature. The scattering intensities (count rates) of PNIPAm$_x$-P123-PNIPAm$_x$

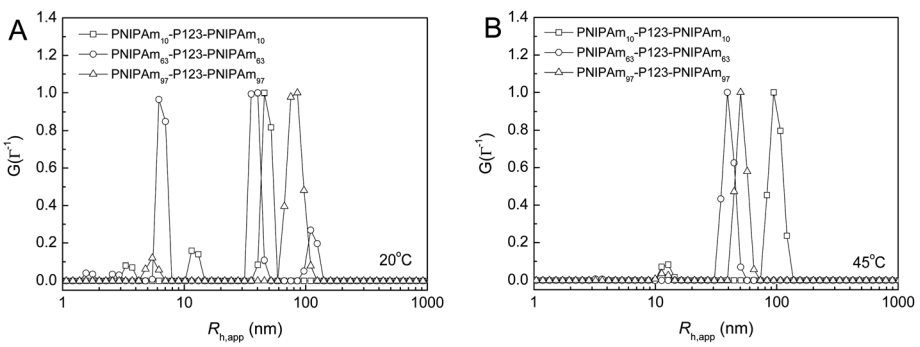

Fig. 3 The distribution of hydrodynamic radius $\langle R_h \rangle$ measured by DLS at scattering angle of 90° for PNIPAm$_x$-P123-PNIPAm$_x$ pentablock terpolymers in aqueous solutions with the concentration of 0.5 mg mL^{-1} at various temperatures (A) 20 °C, and (B) 45 °C.

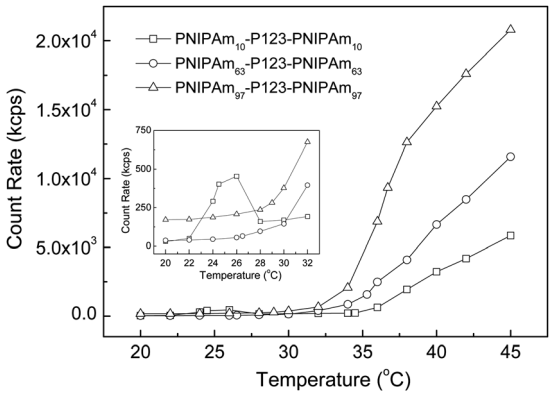

Fig. 4 Scattering intensity (count rate) measured by DLS at scattering angle of 90° for $PNIPAm_x$-P123-$PNIPAm_x$ pentablock terpolymers in dilute aqueous solutions with concentration of 0.5 mg mL^{-1} as a function of temperature. The inset shows the enlarged count rate at low temperature range of 20–32 °C.

pentablock terpolymers in dilute aqueous solutions were fairly weak at 20 °C. The scattering intensities increased with increasing the block length of PNIPAm and were about 30 kcps, 37 kcps, and 171 kcps for $PNIPAm_{10}$-P123-$PNIPAm_{10}$, $PNIPAm_{63}$-P123-$PNIPAm_{63}$, and $PNIPAm_{97}$-P123-$PNIPAm_{97}$, respectively. The weak scattering intensities together with the bimodal size distribution indicate that the pentablock terpolymers adopted single chain conformation and loose ''associate'' structures in the solution at low temperature. Generally speaking, the count rate slowly increased with increasing the temperature for the three $PNIPAm_x$-P123-$PNIPAm_x$ pentablock terpolymers in dilute aqueous solutions from 20 °C to 32 °C as shown in the inset of Fig. 4. Interestingly, a sudden increase was observed at 24 °C for $PNIPAm_{10}$-P123-$PNIPAm_{10}$, which corresponded to the LCST of PPO block. The collapse of PPO block led to the formation of small micelles with hydrophobic PPO block as the core and hydrophilic PNIPAm and PEO blocks as the corona, as shown in Fig. 2. Since $PNIPAm_{10}$-P123-$PNIPAm_{10}$ had the shortest PNIPAm block, the contribution of these small micelles to the scattering intensities was clearly observed. However, for $PNIPAm_{63}$-P123-$PNIPAm_{63}$, and $PNIPAm_{97}$-P123-$PNIPAm_{97}$ with much longer PNIPAm block, no such sudden increase was observed at the LCST of PPO block. The scattering intensity decreased again at 28 °C and then further increased with increasing temperature for $PNIPAm_{10}$-P123-$PNIPAm_{10}$. When the temperature was increased above 34 °C, the count rate increased sharply for the three $PNIPAm_x$-P123-$PNIPAm_x$ pentablock terpolymers and reached as high as 20 800 kcps at 45 °C for $PNIPAm_{97}$-P123-$PNIPAm_{97}$, which strongly indicated the formation of big micelles above 34 °C. Note that 34 °C was the LCST of PNIPAm block. Again, the pentablock terpolymers with longer PNIPAm block had larger scattering intensity at higher temperatures. The hydrodynamic radii $\langle R_h \rangle$ of micelles formed at 45 °C were about 94 nm, 39 nm, and 50 nm for $PNIPAm_{10}$-P123-$PNIPAm_{10}$, $PNIPAm_{63}$-P123-$PNIPAm_{63}$, and $PNIPAm_{97}$-P123-$PNIPAm_{97}$, respectively. Interestingly, the size of $PNIPAm_{10}$-P123-$PNIPAm_{10}$ micelle was much larger than those of $PNIPAm_{63}$-P123-$PNIPAm_{63}$, and $PNIPAm_{97}$-P123-$PNIPAm_{97}$ micelles. One may expect the smaller micelle for block copolymers with shorter hydrophobic blocks. It was true for the diblock copolymer system. Generally, the size of micelle of amphiphilic diblock copolymer formed in selective solvent will increase with increasing the length of hydrophobic block because the longer hydrophobic block forms a larger micelle core. However, for a multiblock copolymer, the situation may be different due to the complex chain architecture. For example, for PNIPAm-P123-PNIPAm pentablock terpolymers studied here, the PNIPAm block had to bend into the hydrophobic PPO core when the temperature was increased above the LCST of PNIPAm, leading to the rearrangement of micelle. The bending and stretching of PNIPAm block in the micelle core and PEO block in the micelle corona cost an energy penalty. Such bending and stretching were easier for longer PNIPAm block, like the cases of $PNIPAm_{63}$-P123-$PNIPAm_{63}$ and $PNIPAm_{97}$-P123-$PNIPAm_{97}$. However, for $PNIPAm_{10}$-P123-$PNIPAm_{10}$ with shortest PNIPAm block, the short PNIPAm block was not easily bent into the micelle core. In order to compensate the energy penalty of bending and stretching and balancing the system free energy, the larger micelle may be formed to decrease the extent of bending and stretching and increase the interface of PEO corona and aqueous phase. This may be the possible reason for the larger size of $PNIPAm_{10}$-P123-$PNIPAm_{10}$ micelle formed at elevated temperature. Further investigations are needed to study the micelle behavior of multiblock copolymer with complex chain structures.

The gyration radii, $\langle R_g \rangle$, of the $PNIPAm_x$-P123-$PNIPAm_x$ pentablock terpolymer micelles formed at 45 °C were also measured by SLS. Fig. 5 shows the Guinier-type plots of Ln $I(q)^{-1} \sim q^2$ measured by SLS for the aqueous solutions of $PNIPAm_x$-P123-$PNIPAm_x$ pentablock terpolymers with concentration of 0.5 mg mL^{-1} at 45 °C. I is the scattering intensity and $q = (4\pi n/\lambda)\sin(\theta/2)$, with λ, n and θ being the wavelength of the laser light in a vacuum (here λ = 632 nm), the refractive index of solvent, and the scattering angle, respectively. The solid lines in Fig. 5 are the linear fits of the data, indicating that the Guinier plot could be used to describe well the SLS data. The radius of gyration, $\langle R_g \rangle$, could be then calculated from the slope of

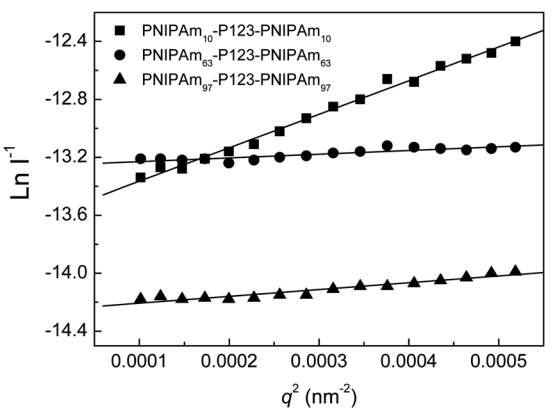

Fig. 5 Guinier-type plots of Ln $I(q)^{-1} \sim q^2$ measured by SLS for the aqueous solutions of $PNIPAm_x$-P123-$PNIPAm_x$ pentablock terpolymers with concentration of 0.5 mg mL^{-1} at 45 °C. The solid lines are linear fits.

$\mathrm{Ln}\, I(q)^{-1} \sim q^2$, *i.e.* $\langle R_g \rangle^2/3$. The radii of gyration, $\langle R_g \rangle$, of the micelles formed at 45 °C were calculated to be 83.3 ± 1.0 nm, 28.0 ± 2.0 nm, and 37.7 ± 1.4 nm for $PNIPAm_{10}$-P123-$PNIPAm_{10}$, $PNIPAm_{63}$-P123-$PNIPAm_{63}$, and $PNIPAm_{97}$-P123-$PNIPAm_{97}$, respectively. The value of $\langle R_g \rangle/\langle R_h \rangle$ can be used to describe the conformation of a polymer chain or the architecture of polymer aggregates in solution or the cross-linking density distribution of the microgels. For example, for linear and flexible polymer chains, $\langle R_g \rangle/\langle R_h \rangle$ is around 1.5, while for uniform hard spheres, $\langle R_g \rangle/\langle R_h \rangle$ is 0.778. The $\langle R_g \rangle/\langle R_h \rangle$ values of 0.886, 0.718 and 0.754 were obtained for $PNIPAm_{10}$-P123-$PNIPAm_{10}$, $PNIPAm_{63}$-P123-$PNIPAm_{63}$, and $PNIPAm_{97}$-P123-$PNIPAm_{97}$ micelles, respectively, which were close to that of the uniform sphere, *i.e.* 0.78. It was understandable because the length of PEO block of $PNIPAm_x$-P123-$PNIPAm_x$ series was only 20. The swollen PEO coronas were short for the micelles of $PNIPAm_x$-P123-$PNIPAm_x$ pentablock terpolymer in the aqueous solutions at 40 °C so that the structures of the micelles were more close to the uniform sphere.

Thermo-sensitive microstructures of pentablock terpolymers in concentrated aqueous solutions

The above experimental results showed that $PNIPAm_x$-P123-$PNIPAm_x$ pentablock terpolymers exhibited two LCSTs in their dilute aqueous solutions, which were dependent on the relative block length of PNIPAm, PPO and PEO blocks. The chain conformation and solution behavior of $PNIPAm_x$-P123-$PNIPAm_x$ pentablock terpolymers in dilute solution were thermo-sensitive. The $PNIPAm_x$-P123-$PNIPAm_x$ pentablock terpolymers could form hydrogels in aqueous solutions with high polymer concentration. Here, we were interested in the effects of relative block lengths and environmental temperatures on the microstructures of the pentablock terpolymer hydrogels formed in concentrated aqueous solution, which were investigated by using synchrotron small angle X-ray scattering (SAXS). The microstructures of PEO-PPO-PEO Pluronics triblock copolymers in concentrated aqueous solutions (hydrogel) as well as their interaction with additives have attracted a lot of attention and have been extensively investigated.[36–46] The SAXS results presented here further showed that the incorporation of thermo-sensitive PNIPAm block with various block lengths strongly affected the microstructures of $PNIPAm_x$-P123-$PNIPAm_x$ hydrogels.

Fig. 6 shows the SAXS profiles for 40 wt% aqueous gels of the P123 and $PNIPAm_x$-P123-$PNIPAm_x$ pentablock terpolymers at room temperature, *i.e.* 26.5 °C at SSRF. For 40 wt% aqueous gel of P123, two series of reflections were observed. The main series of reflections were at $q/q^* \approx 1$, 1.75, 2.01 and 2.65 as relative to the first-order reflection peak centered at 0.437 nm^{-1}, which were consistent with the 1, $\sqrt{3}$, 2, $\sqrt{7}$ sequence and presented a hexagonal packing (hex) of cylindrical micelles. The second series of reflections were at $q/q^* \approx 1$, 1.13, 1.62 and 2.5 as relative to the first-order reflection peak centered at 0.415 nm^{-1}, which were consistent with the 1, $\sqrt{4/3}$, $\sqrt{8/3}$, $\sqrt{19/3}$ sequence and presented a face-centered cubic (fcc) packing of spherical micelles. Such results were in good agreement with previous reports with similar P123 aqueous gels (40 wt%), *i.e.* mixed hex and fcc packings.[40,44] With the incorporation of PNIPAm block, the order structures of aqueous gels were clearly weakened for $PNIPAm_x$-P123-$PNIPAm_x$ pentablock terpolymers. For $PNIPAm_{10}$-P123-$PNIPAm_{10}$, only three reflection peaks were observed at $q/q^* \approx 1$, 1.63, and 1.75 as relative to the first-order peak at 0.400 nm^{-1}, which again indicated the mixed structures of the main hex packing of cylindrical micelles and a portion of fcc packing of spherical micelles. Further increasing the length of PNIPAm block, no order structure was observed for the aqueous gels of $PNIPAm_{63}$-P123-$PNIPAm_{63}$ and $PNIPAm_{97}$-P123-$PNIPAm_{97}$. However, the SAXS patterns showed slightly form factor oscillation. Table 2 lists the gel microstructures, the values of q at the first-order reflection (q^*) and the corresponding d-spacing ($d = 2\pi/q^*$) for 40 wt% aqueous gels of $PNIPAm_x$-P123-$PNIPAm_x$ pentablock terpolymers. It can be seen that the d-spacing increased from 14.4 nm for P123 hydrogel to 15.7 nm for $PNIPAm_{10}$-P123-$PNIPAm_{10}$ hydrogel. However, the presence of short PNIPAm block did not alter the microstructure of P123 gel, which might be possibly due to the pre-existence of mixed microstructure of hex and fcc packings.

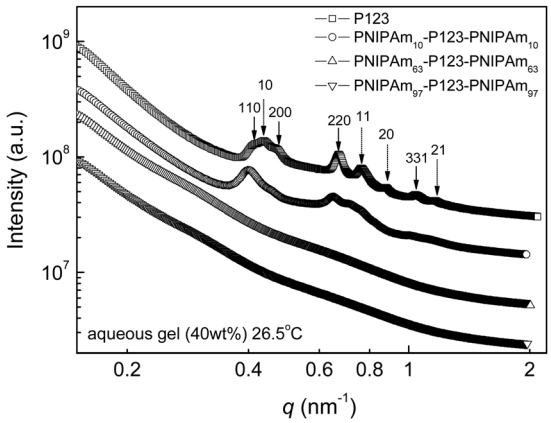

Fig. 6 SAXS profiles for 40 wt% aqueous gels of P123 and $PNIPAm_x$-P123-$PNIPAm_x$ pentablock terpolymers at room temperature, *i.e.* 26.5 °C at SSRF.

Since the $PNIPAm_x$-P123-$PNIPAm_x$ pentablock terpolymers showed thermo-sensitive characters in aqueous solutions, the environmental temperature could also affect the microstructures of their aqueous gels. Fig. 7 shows the SAXS profiles for 40 wt% aqueous gels of P123, $PNIPAm_{10}$-P123-$PNIPAm_{10}$ and $PNIPAm_{97}$-P123-$PNIPAm_{97}$ at various temperatures. For 40 wt% aqueous

Table 2 Structure and d-spacings for the aqueous gels (40 wt%) of $PNIPAm_x$-P123-$PNIPAm_x$ pentablock terpolymers as determined by SAXS

Gel samples	T (°C)	Structure	q^* (nm^{-1})	d (nm)
P123	26.5	Mainly hex	0.437	14.4
	29	Hex	0.423	14.8
	45	Hex	0.397	15.8
$PNIPAm_{10}$-P123-$PNIPAm_{10}$	26.5	Mainly hex	0.400	15.7
	29	Mainly hex	0.406	15.5
	32	Mainly hex	0.401	15.7
	34.5	Hex	0.397	15.8
	38	Hex	0.385	16.3
	45	Hex	0.379	16.6

gel of P123 at 29 °C, the reflections were at $q/q^* \approx 1$, 1.74, and 2.0 relative to the first-order peak centered at 0.423 nm^{-1}, which presented a hexagonal packing (hex) of cylindrical micelles (Fig. 7A). As compared with the SAXS profile for P123 aqueous gel at 26.5 °C, the reflections assigned to the fraction of gel with fcc packing of spherical micelles vanished at 29 °C. Furthermore, the *d*-spacing was 14.8 nm at 29 °C, which was slightly larger than that at 26.5 °C (*i.e.* 14.4 nm). At 45 °C, a hexagonal packing of cylindrical micelles was observed for the P123 aqueous gel (40 wt%) but the *d*-spacing shifted to a much higher value of 15.8 nm (Table 2). These results indicated that the P123 aqueous gel took pure hex packing at higher temperatures, *e.g.* 29 °C and 45 °C, and the *d*-spacing increased with increasing temperatures. For $PNIPAm_{10}$-P123-$PNIPAm_{10}$ aqueous gel, the reflection at $q/q^* \approx 1.63$, which represented the fcc packing of spherical micelles, became weaker and weaker with increasing the temperatures from 26.5 °C to 32 °C and completely vanished at temperatures above 34.5 °C (Fig. 7B). The microstructures of $PNIPAm_{10}$-P123-$PNIPAm_{10}$ aqueous gel mainly consisted of a hexagonal packing (hex) of cylindrical micelles with a fraction of gel with spherical micelles and fcc packing for the temperatures from 26.5 °C to 32 °C. Furthermore, the *d*-spacing was almost the same in the temperature range of 26.5 °C to 32 °C (Table 2). At temperatures $\geq$ 34.5 °C, the aqueous gel of $PNIPAm_{10}$-P123-$PNIPAm_{10}$ took a pure hex packing of cylindrical micelles. Note that 34.5 °C was the second LCST of $PNIPAm_{10}$-P123-$PNIPAm_{10}$ pentablock terpolymer in aqueous solution, which was corresponding to the LCST of PNIPAm block (*cf.* Fig. 1). The *d*-spacing of such hex packing increased from 15.8 nm at 34.5 °C to 16.6 nm at 45 °C, which was similar to the results obtained for P123 aqueous gel with hex packing at high temperatures. The order structures of the $PNIPAm_{10}$-P123-$PNIPAm_{10}$ aqueous gel were weakened with raising temperatures and the first-order reflection even vanished for the aqueous gel at 45 °C (Fig. 7B). The vanishing of the first order reflection might be due to the changes of micelle cross section diameter. The convolution of the structure factor and the micelle form factor may thus significantly affect the diffraction peak intensity, resulting in the vanishing of first-order peak. For $PNIPAm_{97}$-P123-$PNIPAm_{97}$ pentablock terpolymer with the longest PNIPAm block, slight form factor oscillation was observed for the aqueous gel at 26.5 °C. Interestingly, such form factor oscillation became more significant with increasing the temperature (arrow in Fig. 7C).

The above SAXS results indicated that the incorporation of PNIPAm block into P123 triblock copolymers will shift the lyotropic liquid crystalline structures of the 40 wt% aqueous gels from mixed cubic and hexagonal structure to isotropic structure. Increasing temperature will result in the vanishing of cubic structure for P123 and $PNIPAm_{10}$-P123-$PNIPAm_{10}$ aqueous gels, leading to the pure hexagonal structure. These results might be qualitatively correlated and explained in terms of volume fraction, thermo-sensitive block properties, Flory–Huggins interaction parameters and the interfacial curvatures of PPO, PEO and PNIPAm blocks in the aqueous gels. Table 3 shows the calculated volume fraction of water, PPO, PEO and PNIPAm blocks in the 40 wt% aqueous gels for P123 and $PNIPAm_x$-P123-$PNIPAm_x$ pentablock terpolymers. Note that the molar masses of the PO, EO, and NIPAm monomer were 58 g mol^{-1}, 44 g mol^{-1}, and 113.2 g mol^{-1}, respectively.

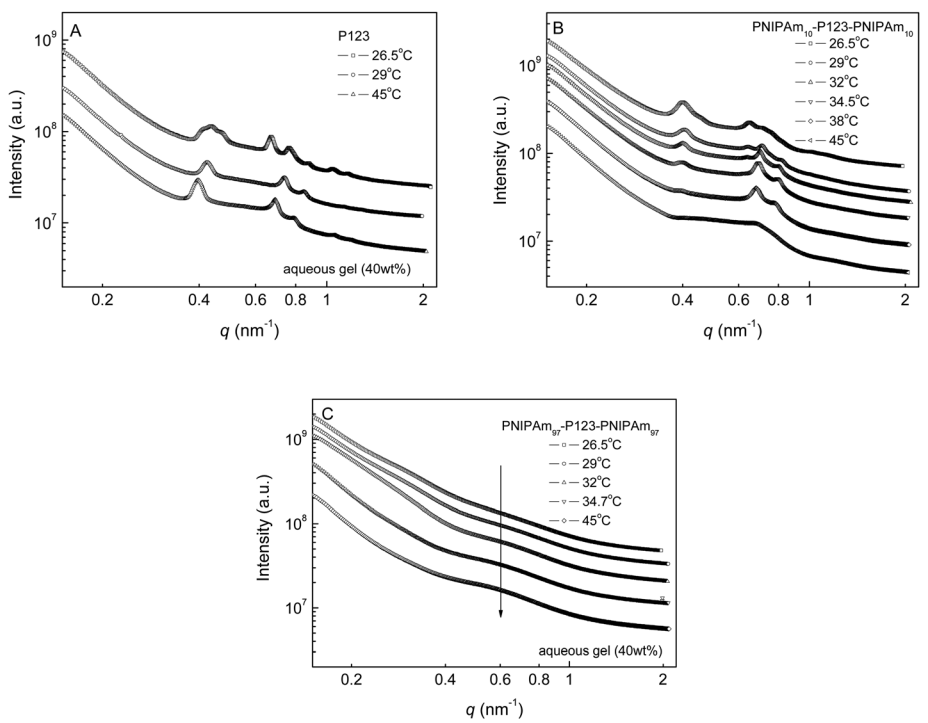

Fig. 7 SAXS profiles for 40 wt% aqueous gels of (A) P123, (B) $PNIPAm_{10}$-P123-$PNIPAm_{10}$ and (C) $PNIPAm_{97}$-P123-$PNIPAm_{97}$ at various temperatures.

Table 3 Volume fractions of H_2O, PEO, PPO and PNIPAm in the 40 wt% aqueous gels

Gel samples	f_{H_2O}	f_{PEO}	f_{PPO}	f_{PNIPAm}
P123	0.60	0.121	0.279	—
$PNIPAm_{10}$-P123-$PNIPAm_{10}$	0.609	0.087	0.202	0.101
$PNIPAm_{63}$-P123-$PNIPAm_{63}$	0.619	0.039	0.082	0.263
$PNIPAm_{97}$-P123-$PNIPAm_{97}$	0.621	0.026	0.060	0.293

The densities of the PO, EO, and NIPAm monomers were 1.01 g cm^{-3}, 1.01 g cm^{-3}, and 1.115 g cm^{-3}, respectively.[47,48]

The phase behavior of block copolymer is determined by the competition between interfacial tension and the entropic penalty for stretching polymer chains so as to fill space uniformly. The interfacial curvature allows the molecules to balance the degree of stretching among the blocks.[49] For amphiphilic block copolymer with apolar and polar components, the interfacial curvature is defined as positive when the interface bends toward the apolar domains. For the lamellar or isotropic structure, the interfacial curvature is zero. The shift from cubic to hexagonal structure suggested the decrease of interfacial curvature with increasing the block length of PNIPAm block. With increasing the block length x of PNIPAm block, the interfacial curvature changed from positive (for P123 with mixed fcc and hex structure with x = 0) to intermediately positive (for $PNIPAm_{10}$-P123-$PNIPAm_{10}$ with mixed hexagonal and fcc structure) to zero (for $PNIPAm_{97}$-P123-PNIPAm$_{97}$ with longest PNIPAm block and isotropic structure). Increasing temperature also led to the decrease of interfacial curvature, leading to the transition from mixed hex and fcc structure to pure hex structure for $PNIPAm_{10}$-P123-$PNIPAm_{10}$ aqueous gel at elevated temperature above 34.5 °C.

The phase behavior and structures of linear ABC triblock terpolymer co-assemblies are rather complex and governed at least by five parameters: two independent volume fractions, f_a and f_b, and three products of the Flory–Huggins parameter (χ) with the overall degree of polymerization (N): $\chi_{AB}N$, $\chi_{BC}N$, and $\chi_{CA}N$.[50–52] However, for CBABC pentablock terpolymer aqueous gel, more parameters will determine the final structure of the aqueous gel. One has to consider at least other three parameters for a given concentration of CBABC pentablock terpolymer aqueous gel, *i.e.*χ_{AS}, χ_{BS}, and χ_{CS}, where S presents the solvent. For $PNIPAm_x$-P123-$PNIPAm_x$ aqueous gels, the closest example was the self-assembly of $PDEAEM_{25}$-F127-$PDEAEM_{25}$ pentablock terpolymer in aqueous solution reported by the Mallapragada group, where PDEAEM was poly(diethylaminoethyl methacrylate).[2] The authors found that $PDEAEM_{25}$-F127-$PDEAEM_{25}$ precipitated and coalesced into a hydrogel structure with 25–35 wt% water at pH > 11.[2] SAXS clearly indicated that the hydrogel had a hexagonal ordered phase of cylindrical micelles with a d spacing of 15.1 nm.[2] Note that PDEAEM block was hydrophobic at pH > 11.[2] For $PNIPAm_x$-P123-$PNIPAm_x$ pentablock terpolymer, the Flory–Huggins parameters, $\chi_{PPO/PEO}$, $\chi_{PPO/PNIPAm}$, and $\chi_{PEO/PNIPAm}$ could be estimated by using the approximation by Hildebrand and Scott:[53]

$$\chi_{AB} = \frac{v_{ref}(\delta_A - \delta_B)^2}{RT} \quad (1)$$

where v_{ref} is the segment reference volume and δ_A is the Hildebrand solubility parameter of polymer A. The segment reference volume v_{ref} is approximated as $v_{ref} = (v_A v_B)^{1/2}$, with v_A and v_B for the specific volumes of polymers A and B. The specific volumes of polymers were obtained as the ratios of the monomer molecular weight to their densities. The solubility parameters of PEO and PPO were δ_{PEO} = 20.2 (J cm^{-3})$^{1/2}$ and δ_{PPO} = 15.4 (J cm^{-3})$^{1/2}$, respectively.[54] The solubility parameter for PNIPAm could be calculated by $\delta = \rho\sum G/M$, where ρ is the density of the monomer NIPAm (1.115 g cm^{-3}), G is the group molar attraction constant for each of the constituent chemical groups in the polymer, and M is the molecular weight of monomer NIPAm (113.2 g mol^{-1}). The solubility parameter of PNIPAm was then calculated to be δ_{PNIPAm} = 18.5 (J cm^{-3})$^{1/2}$. Although there were polar interactions between such hydrophilic polymers and the water, the estimation of χ parameters from eqn (1) with solubility parameters still provided us the preliminary understanding of the microstructure evolution of $PNIPAm_x$-P123-$PNIPAm_x$ hydrogels as a function of temperature.

At room temperature of 26.5 °C, the Flory–Huggins parameters, $\chi_{PPO/PEO}$, $\chi_{PPO/PNIPAm}$, and $\chi_{PEO/PNIPAm}$ were then estimated to be 0.462, 0.295 and 0.077, respectively. It can be seen that PNIPAm phase is more compatible with PEO phase and PPO phase tends to phase separation from PEO phase. According to the calculated χ parameter, PNIPAm phase might tend to locate between the PPO and PEO phases in order to minimize the PPO-PEO interface, leading to the decrease of interfacial curvature between the polar and apolar domains. Increasing the length of PNIPAm block (the volume fraction of PNIPAm block) will further decrease the interfacial curvature. This might be a possible reason why the hydrogel structure changed from mixed hex and fcc structure to isotropic structure with increasing x = 0 for P123 to x = 97 for $PNIPAm_{97}$-P123-$PNIPAm_{97}$.

Interestingly, for P123 and $PNIPAm_{10}$-P123-$PNIPAm_{10}$ with short PNIPAm block (x = 10), the packing structures of hydrogels changed from mixed hex and fcc to pure hex structure with increasing temperature. For $PNIPAm_{97}$-P123-PNIPAm$_{97}$ aqueous gel, the form factor oscillation became more significant with increasing temperature. The solubility of water is 48.0 (J cm^{-3})$^{1/2}$, which is much larger than those of PPO, PEO, and PNIPAm. According to the theoretical calculation of eqn (1), PPO, PEO, and PNIPAm were expected to have large Flory–Huggins parameters, χ, and be hence less soluble in water. In reality, PPO, PEO, and PNIPAm are soluble in water at low temperature below their LCSTs due to the specific interactions of hydrogen bonding between the polymer and water. Increasing the temperature will destroy the hydrogen bonding, leading to the thermo-sensitive characters for PPO, PEO, and PNIPAm in aqueous solutions. At high temperature, PPO and PNIPAm blocks became hydrophobic. Furthermore, the segregation between the PEO and PPO decreased with increasing temperature.[55] The interfacial curvature decreased with increasing temperature. The interfacial curvature, which was requested for achieving a uniform packing of micelle, was dependent on the volume fractions of polar and apolar components. With increasing the temperature, PNIPAm blocks became

hydrophobic. At temperature above its LCST, PNIPAm fraction changed from partial polar component to fully apolar component. The apolar component of PNIPAm-PEO-PPO-PEO-PNIPAm pentablock terpolymer hence strongly increased with increasing temperature, leading to the decrease of interfacial curvature. Table 2 also shows that the lattice parameter (corresponding to the d-spacing of q^*) of the hexagonal structure increased with increasing temperature for P123 and PNIPAm$_{10}$-P123-PNIPAm$_{10}$ hydrogels, which was similar with those observed for Pluronic P84 (PEO_{19}-PPO_{43}-PEO_{19}) in p-xylene.[55] The interfacial area of polar/apolar interface, which was widely applied in the interpretation of SAXS data of PEO-PPO-PEO triblock copolymer, might be utilized to semi-quantitatively describe the phase separation of PNIPAm-PEO-PPO-PEO-PNIPAm pentablock terpolymer. The interfacial area per PEO block, a_p, which presents a PEO block of the PEO-PPO-PEO triblock copolymer occupying the interface between polar and apolar domains, could be calculated by[37]

$$a_p = \frac{v_p}{d\Phi_p}\left(\frac{\pi\sqrt{3}}{2}f\right)^{1/2} \quad \text{for hexagonal structure} \qquad (2)$$

where v_p is the volume of one macromolecule, f is the apolar volume fraction and Φ_p is the volume fraction of the copolymer in the hydrogel system. However, it was worthy to point it out that eqn (2) might be not suitable for describing the phase behavior of the terpolymer systems like the CBABC pentablock terpolymer studied here. Nevertheless, from eqn (2), the increase of d-spacing for P123 and PNIPAm$_{10}$-P123-PNIPAm$_{10}$ hydrogels with hexagonal structure suggested the decrease of polar/apolar interface area, which was consistent with the fact that the segregation among the PEO, PPO and PNIPAm blocks decreased with increasing temperature. The preliminary results reported in the present work showed that the aqueous gels of thermosensitive PNIPAm$_x$-P123-PNIPAm$_x$ pentablock terpolymers exhibited rich phase structures, depending on the length of PNIPAm block and the environmental temperature. The chain structure of the CBABC pentablock terpolymers were much more complex than those of AB and ABA block copolymers as well as ABC triblock terpolymer, more experimental investigations and theoretical treatments are still needed to elucidate the phase behavior of the PNIPAm$_x$-P123-PNIPAm$_x$ pentablock terpolymers. The effects of PNIPAm polymer on the microstructures of P123 hydrogel might be also investigated for comparison in future.

Conclusions

The relative block lengths of PNIPAm, PPO, and PEO blocks had significant effects on the solution behavior and microstructure of PNIPAm$_x$-P123-PNIPAm$_x$ pentablock terpolymers in dilute and concentrated aqueous solutions. The PNIPAm$_x$-P123-PNIPAm$_x$ pentablock terpolymers exhibited two LCSTs, which were corresponding to LCSTs of PPO and PNIPAm blocks, respectively. The LCST of PPO block shifted from 24.4 °C to 29 °C when the length x of PNIPAm block increased from 10 to 97. The LCST of PNIPAm is around 34.5–35.3 °C and less dependent on the block length x. The PNIPAm$_x$-P123-PNIPAm$_x$ pentablock terpolymers formed ''associate'' structures and micelles with hydrophobic PNIPAm and PPO blocks as cores and soluble PEO blocks as coronas in the dilute aqueous solution at temperatures well below and above the LCSTs of the PPO and PNIPAm blocks, respectively, regardless of the relative lengths of PNIPAm, PPO and PEO blocks. The microstructures of PNIPAm$_x$-P123-PNIPAm$_x$ hydrogels formed in concentrated aqueous solutions (40 wt%) were strongly dependent on the environmental temperatures and relative lengths of PNIPAm, PPO and PEO blocks as revealed by SAXS. Increasing the block length x of PNIPAm block decreased the interfacial curvature of polar/apolar interface. The interfacial curvature changed from positive (for P123 and PNIPAm$_{10}$-P123-PNIPAm$_{10}$ with mixed hexagonal and fcc structure) to zero (for PNIPAm$_{63}$-P123-PNIPAm$_{63}$ and PNIPAm$_{97}$-P123-PNIPAm$_{97}$ with isotropic structure). Increasing the environmental temperature also led to the decrease of interfacial curvature, leading to the transition of mixed hex and fcc structure to pure hex structure for PNIPAm$_{10}$-P123-PNIPAm$_{10}$ aqueous gel at elevated temperature above the LCST of PNIPAm block, *i.e.* 34.5 °C.

Acknowledgements

We thank the National Natural Science Foundation of China (Nos. 21074114 and 21274129) for financial supports. We thank Prof. Qiang Zheng for the use of BI-200SM. We thank BL16B1 beamline at Shanghai Synchrotron Radiation Facility (SSRF) for providing the beam time (No.10sr0475).

Notes and references

1 S. Bhattacharya, H. P. Hsu, A. Milchev, V. G. Rostiashvili and T. A. Vilgis, *Macromolecules*, 2008, **41**, 2920.
2 M. D. Determan, L. Guo, P. Thiyagarajan and S. K. Mallapragada, *Langmuir*, 2006, **22**, 1469.
3 B. Y. Du, A. X. Mei, Y. Yang, Q. F. Zhang, Q. Wang, J. T. Xu and Z. Q. Fan, *Polymer*, 2010, **51**, 3493.
4 M. E. Gindy, R. K. Prud'homme and A. Z. Panagiotopoulos, *J. Chem. Phys.*, 2008, **128**, 13.
5 J. Hong, Q. Wang, Y. Z. Lin and Z. Q. Fan, *Macromolecules*, 2005, **38**, 2691.
6 L. Z. Hong, F. M. Zhu, J. F. Li, T. Ngai, Z. W. Xie and C. Wu, *Macromolecules*, 2008, **41**, 2219.
7 V. Hugouvieux, M. A. V. Axelos and M. Kolb, *Macromolecules*, 2009, **42**, 392.
8 J. S. Lintuvuori and M. R. Wilson, *Phys. Chem. Chem. Phys.*, 2009, **11**, 2116.
9 Y. P. Lu, X. H. Zhang, Z. Q. Fan and B. Y. Du, *Polymer*, 2012, **53**, 3791.
10 L. S. Zhang, Q. Wang, P. Lei, X. Wang, C. Y. Wang and L. Cai, *J. Polym. Sci., Part A: Polym. Chem.*, 2007, **45**, 2617.
11 Y. M. Zhou, K. Q. Jiang, Q. L. Song and S. Y. Liu, *Langmuir*, 2007, **23**, 13076.
12 B. Y. Du, A. X. Mei, K. Z. Yin, Q. F. Zhang, J. T. Xu and Z. Q. Fan, *Macromolecules*, 2009, **42**, 8477.

13 X. N. Huang, F. S. Du, J. Cheng, Y. Q. Dong, D. H. Liang, S. P. Ji, S. S. Lin and Z. C. Li, *Macromolecules*, 2009, **42**, 783.
14 J. Kriz and J. Dybal, *J. Phys. Chem. B*, 2010, **114**, 3140.
15 L. B. Luo and A. Eisenberg, *J. Am. Chem. Soc.*, 2001, **123**, 1012.
16 G. Riess, *Prog. Polym. Sci.*, 2003, **28**, 1107.
17 E. B. Zhulina, M. Adam, I. LaRue, S. S. Sheiko and M. Rubinstein, *Macromolecules*, 2005, **38**, 5330.
18 M. D. Determan, J. P. Cox, S. Seifert, P. Thiyagarajan and S. K. Mallapragada, *Polymer*, 2005, **46**, 6933.
19 N. A. Hadjiantoniou, T. Krasia-Christoforou, E. Loizou, L. Porcar and C. S. Patrickios, *Macromolecules*, 2010, **43**, 2713.
20 N. A. Hadjiantoniou, A. I. Triftaridou, D. Kafouris, M. Gradzielski and C. S. Patrickios, *Macromolecules*, 2009, **42**, 5492.
21 T. Harada, F. S. Bates and T. P. Lodge, *Macromolecules*, 2003, **36**, 5440.
22 A. X. Mei, X. L. Guo, Y. W. Ding, X. H. Zhang, J. T. Xu, Z. Q. Fan and B. Y. Du, *Macromolecules*, 2010, **43**, 7312.
23 S. Peleshanko, K. D. Anderson, M. Goodman, M. D. Determan, S. K. Mallapragada and V. V. Tsukruk, *Langmuir*, 2007, **23**, 25.
24 K. Sha, D. S. Li, Y. P. Li, B. Zhang and J. Y. Wang, *Macromolecules*, 2008, **41**, 361.
25 R. F. Storey, A. D. Scheuer and B. C. Achord, *Polymer*, 2005, **46**, 2141.
26 C. Tsitsilianis, N. Stavrouli, V. Bocharova, S. Angeiopouios, A. Kiriy, I. Katsampas and M. Stamm, *Polymer*, 2008, **49**, 2996.
27 L. F. Wu, E. W. Cochran, T. P. Lodge and F. S. Bates, *Macromolecules*, 2004, **37**, 3360.
28 Y. He and T. P. Lodge, *Macromolecules*, 2008, **41**, 167.
29 P. Alexandridis, J. F. Holzwarth and T. A. Hatton, *Macromolecules*, 1994, **27**, 2414.
30 X. P. Qiu, C. M. S. Kwan and C. Wu, *Macromolecules*, 1997, **30**, 6090.
31 X. P. Qiu and C. Wu, *Macromolecules*, 1997, **30**, 7921.
32 H. G. Schild, *Prog. Polym. Sci.*, 1992, **17**, 163.
33 Y. F. Wu, X. L. Liu, Y. Wang, Z. R. Guo and Y. J. Feng, *Macromol. Chem. Phys.*, 2012, **213**, 1489.
34 F. Y. Ke, X. L. Mo, R. M. Yang, Y. M. Wang and D. H. Liang, *Macromolecules*, 2009, **42**, 5339.
35 J. J. Yan, W. X. Ji, E. Q. Chen, Z. C. Li and D. H. Liang, *Macromolecules*, 2008, **41**, 4908.
36 P. Alexandridis, R. Ivanova and B. Lindman, *Langmuir*, 2000, **16**, 3676.
37 P. Alexandridis, U. Olsson and B. Lindman, *Langmuir*, 1998, **14**, 2627.
38 P. Alexandridis, D. L. Zhou and A. Khan, *Langmuir*, 1996, **12**, 2690.
39 C. Chaibundit, N. Ricardo, N. Ricardo, F. Costa, M. G. P. Wong, D. Hermida-Merino, J. Rodriguez-Perez, I. W. Hamley, S. G. Yeates and C. Booth, *Langmuir*, 2008, **24**, 12260.
40 C. Chaibundit, N. Ricardo, N. Ricardo, B. M. D. O'Driscoll, I. W. Hamley, S. G. Yeates and C. Booth, *Langmuir*, 2009, **25**, 13776.
41 S. dos Santos, B. Luigjes and L. Piculell, *Soft Matter*, 2010, **6**, 4756.
42 R. Ivanova, B. Lindman and P. Alexandridis, *Langmuir*, 2000, **16**, 9058.
43 R. Ivanova, B. Lindman and P. Alexandridis, *Langmuir*, 2000, **16**, 3660.
44 K. Mortensen, W. Batsberg and S. Hvidt, *Macromolecules*, 2008, **41**, 1720.
45 S. S. Soni, G. Brotons, M. Bellour, T. Narayanan and A. Gibaud, *J. Phys. Chem. B*, 2006, **110**, 15157.
46 G. Wanka, H. Hoffmann and W. Ulbricht, *Macromolecules*, 1994, **27**, 4145.
47 G. M. Mao, S. Sukumaran, G. Beaucage, M. L. Saboungi and P. Thiyagarajan, *Macromolecules*, 2001, **34**, 552.
48 J. J. Nie, B. Y. Du and W. Oppermann, *Macromolecules*, 2004, **37**, 6558.
49 M. W. Matsen and F. S. Bates, *Macromolecules*, 1996, **29**, 7641.
50 G. G. du Sart, R. Rachmawati, V. Voet, G. A. van Ekenstein, E. Polushkin, G. ten Brinke and K. Loos, *Macromolecules*, 2008, **41**, 6393.
51 H. Huckstadt, A. Gopfert and V. Abetz, *Polymer*, 2000, **41**, 9089.
52 R. Stadler, C. Auschra, J. Beckmann, U. Krappe, I. Voigtmartin and L. Leibler, *Macromolecules*, 1995, **28**, 3080.
53 J. H. Hildebrand and R. L. Scott, *The solubility of Non-Electrolytes*, Reinhold, New York, 1949; T. M. Madkour, *Chem. Phys.*, 2001, **274**, 187.
54 S. Michielsen, in *Polymer Handbook*, ed. J. Brandrup and E. H. Immergut, John Wiley & Sons, New York, 3rd edn, 1989, ch. VII, pp. 554–555.
55 B. Svensson and U. Olsson, *Macromolecules*, 2000, **33**, 7413.

